A role for fast rhythmic bursting neurons in cortical gamma oscillations *in vitro*

Mark O. Cunningham*, Miles A. Whittington*†, Andrea Bibbig‡, Anita Roopun*, Fiona E. N. LeBeau*, Angelika Vogt§, Hannah Monyer§, Eberhard H. Buhl*¶, and Roger D. Traub‡‖

*School of Biomedical Sciences, The Worsley Building, University of Leeds, Leeds LS2 9JT, United Kingdom; ‡Department of Physiology and Pharmacology, State University of New York Downstate Medical Center, 450 Clarkson Avenue, Box 31, Brooklyn, NY 11203; and §Department of Clinical Neurobiology, University Hospital of Neurology, Im Neuenheimer Feld 364, 69120 Heidelberg, Germany

Communicated by Nancy J. Kopell, Boston University, Boston, MA, March 24, 2004 (received for review January 19, 2004)

Basic cellular and network mechanisms underlying gamma frequency oscillations (30–80 Hz) have been well characterized in the hippocampus and associated structures. In these regions, gamma rhythms are seen as an emergent property of networks of principal cells and fast-spiking interneurons. In contrast, in the neocortex a number of elegant studies have shown that specific types of principal neuron exist that are capable of generating powerful gamma frequency outputs on the basis of their intrinsic conductances alone. These fast rhythmic bursting (FRB) neurons (sometimes referred to as ''chattering'' cells) are activated by sensory stimuli and generate multiple action potentials per gamma period. Here, we demonstrate that FRB neurons may function by providing a large-scale input to an axon plexus consisting of gap-junctionally connected axons from both FRB neurons and their anatomically similar counterparts regular spiking neurons. The resulting network gamma oscillation shares all of the properties of gamma oscillations generated in the hippocampus but with the additional critical dependence on multiple spiking in FRB cells.

Gamma frequency oscillations are readily recordable from scalp and depth electroencephalogram electrodes placed over or in the neocortex of humans and laboratory animals. They occur spontaneously at low amplitude or transiently at larger amplitudes in response to sensory stimuli (1, 2). Their role in processing of sensory information has been proposed to involve the establishment of a temporal framework within which long-range synchronization of individual neuronal elements coding for specific sensory events can occur (3). Qualitatively similar oscillations also occur in the hippocampus (4) and entorhinal cortex (5), where their generation can be ascribed to the phasic or tonic (or a combination of both) excitation of fast spiking (FS) interneurons, the outputs of which, in turn, provide a temporal framework for controlling the outputs of principal cells (6, 7).

Although much is known of the mechanisms underlying gamma oscillations in the archicortex and entorhinal cortex, relatively little evidence is available to suggest a mechanism (or mechanisms) involved in generating neocortical gamma oscillations. What is known is that specific neurons exist within the neocortical mantle that are capable of generating outputs within the gamma frequency range on the basis of intrinsic properties alone (in the absence of influences from local networks). Such neurons exhibit fast rhythmic bursting (FRB), with interburst frequencies of 20 Hz and upward, in response to depolarizing current injection alone (8–10). These FRB neurons (sometimes called ''chattering cells'') have also been shown to participate in visually evoked gamma (25–70 Hz) oscillations *in vivo* (8), with the FRB cells morphologically identified as spiny layer II/III pyramidal neurons. Other principal neocortical neurons also possess the ability to generate activity within the gamma band on the basis of intrinsic properties alone in layer IV (11), and some interneurons also demonstrate this ability (9).

A number of similar types of interneuron exist in neo- and archicortex, and phenomena associated with gap junctional activity within principal cell networks has been shown in neocortex (12, 13). It therefore appears that all of the components shown to be important in generating archicortical gamma also exist in neocortex alongside the above intrinsic gamma generators. Here, we used an experimental *in vitro* model of cortical gamma oscillations and network simulations to investigate how FRB neurons could contribute mechanistically to gamma oscillations. Specifically, we investigated whether these neurons were necessary for neocortical gamma oscillations and how they would interact with phylogenetically older network mechanisms of gamma rhythmogenesis.

Methods

Slice Methods. Horizontal 450-μm-thick slices were prepared from adult male Wistar rats (150–250 g). Neocortical slices containing primary and secondary auditory areas and secondary parietal areas were maintained at 34°C at the interface between warm wetted 95% O_2/5% CO_2 and artificial cerebrospinal fluid containing (in mM): 3 KCl, 1.25 NaH_2PO_4, 1 $MgSO_4$, 1.2 $CaCl_2$, 24 $NaHCO_3$, 10 glucose, and 126 NaCl. Extracellular recordings from primary auditory cortex were obtained by using glass micropipettes containing the above artificial cerebrospinal fluid (resistance <0.5 MΩ). Intracellular recordings were taken with sharp microelectrodes filled with potassium acetate (resistance 30–90 MΩ). Signals were analogue filtered at 2 kHz and digitized at 10 kHz. All neuronal recordings illustrated were taken from layer III (including layer II/III and layer III/IV borders).

Simulation Methods. The network model contains 1,152 pyramidal cells, 192 FS (fast-spiking) interneurons, and 96 LTS (low-threshold spiking) interneurons. The proportions of pyramidal cells which were RS (regular spiking), or FRB were varied between simulations. RS and FS cells did not have any intrinsic capability of generating gamma frequency outputs. There are chemical synaptic interactions mediated by α-amino-3-hydroxy-5-methyl-4-isoxazolepropionic acid (AMPA)/kainate receptors and γ-aminobutyric acid type A ($GABA_A$) receptors, as well as electrical coupling between the axons of some of the pyramidal cells and the dendrites of some of the interneurons. Half of the FS interneurons are basket cells, synaptically contacting the soma and proximal dendrites of pyramidal cells; the other half of the FS interneurons are axoaxonic (chandelier) cells, contacting the most proximal axon of pyramidal cells, and not synaptically contacting any interneurons. Connections, both synaptic and electrical, were formed randomly, so far as the identity of cells was concerned; that is, the spatial location of cell

Abbreviations: FRB, fast rhythmic bursting; FS, fast spiking; LTS, low-threshold spiking; RS, regular spiking; AMPA, α-amino-3-hydroxy-5-methyl-4-isoxazolepropionic acid; $GABA_A$, γ-aminobutyric acid type A; EPSP, excitatory postsynaptic potential.

†To whom correspondence should be addressed for questions on electrophysiology. E-mail: m.a.whittington@leeds.ac.uk

¶Deceased January 18, 2003.

‖To whom correspondence should be addressed. E-mail: roger.traub@downstate.edu.

www.pnas.org/cgi/doi/10.1073/pnas.0402060101

bodies was not considered. On the other hand, there were constraints as to where on each neuron particular sorts of connections were allowed to form. Further simulation details can be found in *Supporting Text*, further information on properties of pyramidial cells can be found in Fig. 5, characteristics of interneurons can be found in Fig. 6 and Table 1, which are published as supporting information on the PNAS web site.

***In Situ* Hybridization Methods.** Adult female rats were anesthetized and perfused with 4% paraformaldehyde in phosphate buffer (pH 7.4). Brains were removed and postfixed overnight at 4°C before 50-μm-thick sections were cut. *In situ* hybridization was performed by using sense (control) and antisense RNAs for Px2. DNA templates for px2 spanned the entire ORF (14) and were cloned into pBluescript SK−. For riboprobe synthesis, the recombinant plasmids were linearized and *in vitro* transcription was performed with T3(sense) and T7(antisense) polymerase. Riboprobes were purified by using miniquick-spin RNA columns (Roche Diagnostics, Mannheim, Germany) and stored at −70°C. *In situ* hybridization was performed as described in ref 15.

Results

We produced persistent field potential gamma oscillations in rat auditory cortex slices, in an interface slice preparation, by adding 400 nM kainate to the bathing medium (Fig. 1*A*). Power spectra, obtained through different layers in the cortex, indicated that the maximum gamma power occurred approximately in layer III. The oscillations persisted for hours, as has been reported for other *in vitro* preparations, including carbachol/kainate oscillations in cortex (16), carbachol oscillations in hippocampus (17), and kainate oscillations in hippocampus (18, 19). For persistent hippocampal oscillations, driven by kainate application, the rhythm appears to be generated as a consequence of a large increase in ectopic spike generation within an axon plexus. These spikes drive large compound, phasic, AMPA receptor-mediated excitatory postsynaptic potentials (EPSPs) to FS interneurons which, in turn, feed back onto principal cells to modulate axonal activity (19).

To analyze *in vitro* cortical gamma oscillations, we constructed a network simulation model of layers II/III, by using four types of multicompartment neurons: RS and FRB pyramidal cells (modeled as in ref. 20, with 1,152 pyramidal neurons in all, having a variable proportion of FRB cells); 192 FS interneurons, divided between basket cells and axoaxonic cells; and 96 LTS interneurons, which contacted dendrites of other cells. FRB cells were distinguished from RS cells by being more depolarized, having greater persistent g_{Na} density, and fewer BK channels (20). The cells were interconnected synaptically, through AMPA and $GABA_A$ receptors, and by means of electrical coupling. Electrical coupling occurred between the axons of principal cells, as in our models of hippocampal persistent gamma (21); between the dendrites of FS cells; and between the dendrites of LTS cells (22–25). Further structural details are in *Supporting Text*. The network generated gamma oscillations in the presence of a low frequency (1 Hz per axon) of ectopic spikes in pyramidal cell axons (26). In control simulations, 5% of pyramidal cells were FRB. In "wiring" the model, both for synaptic and also electrical connections, no distinction was made in the simulation program between RS and FRB cells.

The network model and cortical slice oscillations shared a qualitatively similar "pharmacology." In the model, blocking electrical coupling, or AMPA receptors, or $GABA_A$ receptors, all reduced peak gamma power 500-fold, while prolonging $GABA_A$ decay time constant 2-fold reduced the peak frequency from 34.8 to 26.9 Hz. Experimentally, the gap-junction blocker carbenoxolone (0.1 mM) reduced gamma power (from layer III) 2.4-fold (control 6.4 ± 2.7 nV^2 Hz, carbenoxolone 2.6 ± 1.3 nV^2 Hz, $n = 5$); the specific AMPA receptor blocker SYM2206 (10

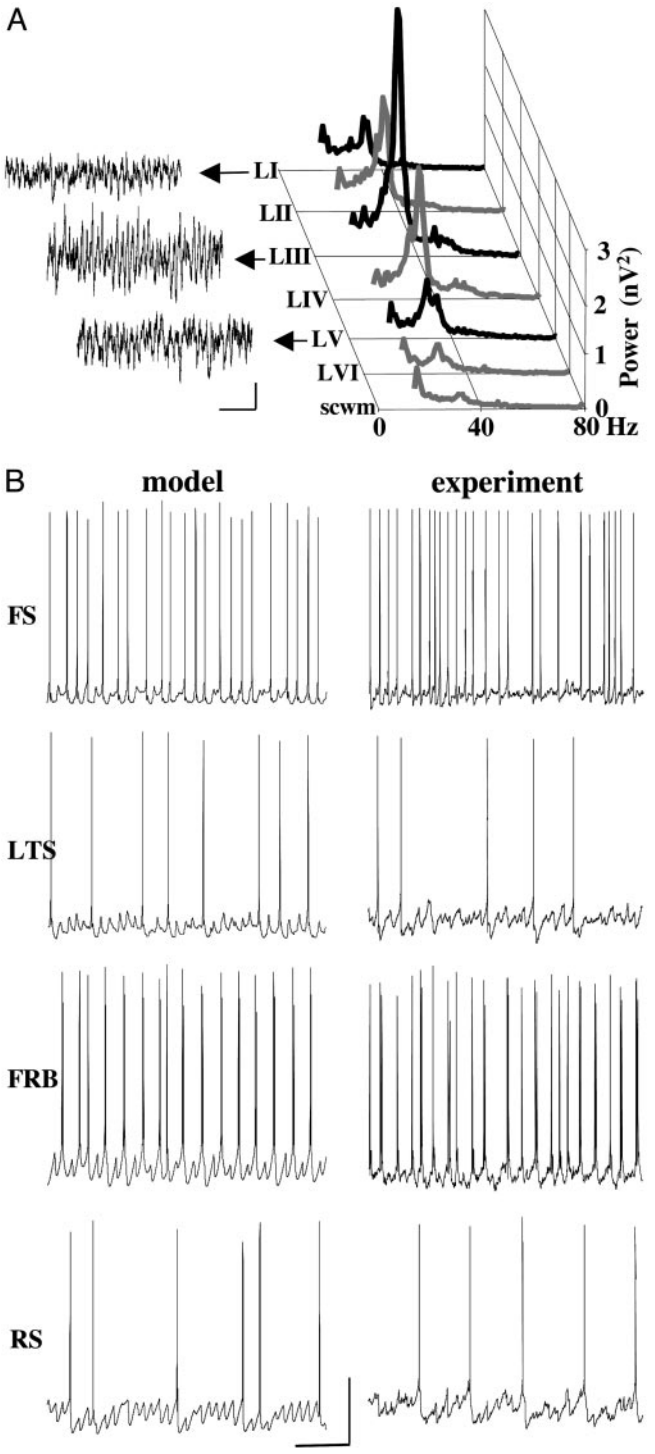

Fig. 1. Kainate-induced gamma oscillations in rat auditory cortex *in vitro*. (*A*) Mean power spectra (60-s epochs, $n = 10$ slices) of persistent field oscillatory activity generated by bath application of 400 nM kainate. The maximum field gamma power was found in layer III (mean frequency 33 ± 4 Hz). Scwm, subcortical white matter. Sample field potentials from layers I, III, and V are shown on the left (scale bars: 50 μV, 200 ms). (*B*) Firing patterns of the different neuronal cell types are similar in the network model and *in vitro* experiments. Data show 1-s epochs of activity. In each case, FS interneurons fire on the majority of the waves. LTS interneurons fire on a minority of the waves, with subthreshold synaptic potentials clearly visible. FRB cells fire on approximately half the waves, usually in spike multiplets, and with synaptic potentials visible between spikes (Note that FRB spike patterns were not stereotyped, consisting of one to four spikes per active phase; e.g., see also Fig. 3). RS pyramidal cells fire sparsely, again with clearly visible synaptic potentials. Scale bars: 25 mV, 200 ms.

μM) reduced it 6.2-fold (control 7.0 $\pm$ 3.1 nV^2 Hz, SYM2206 1.1 $\pm$ 0.3 nV^2 Hz, $n = 5$); bicuculline (10 μM) reduced it 6.0-fold (control 1.2 $\pm$ 0.3 nV^2 Hz, bicuculline 0.2 $\pm$ 0.2 nV^2 Hz, $n = 5$); and pentobarbital (20 μM) reduced the peak frequency from 33 $\pm$ 4 Hz to 20 $\pm$ 2 Hz ($n = 6$); all with $P < 0.05$.

Firing patterns of the various cell types, presumably recorded in the soma, were also strikingly similar, comparing model with experiment (Fig. 1*B*). FS cells fired on the highest proportion of field gamma periods (28.5 Hz average firing rate in two model FS cells, overall model oscillation frequency 34.8 Hz), whereas LTS firing was sparser (15.5 Hz average firing rate in two model LTS cells). FRB cells either skipped periods, or fired a spike singlet, doublet, or triplet; in the model, two FRB cells fired a spike or a doublet at 17 Hz, i.e., on 50% of the waves. RS cells fired sparsely (8.8 Hz average rate in 12 model cells), but with clear subthreshold gamma oscillation consisting of synaptic

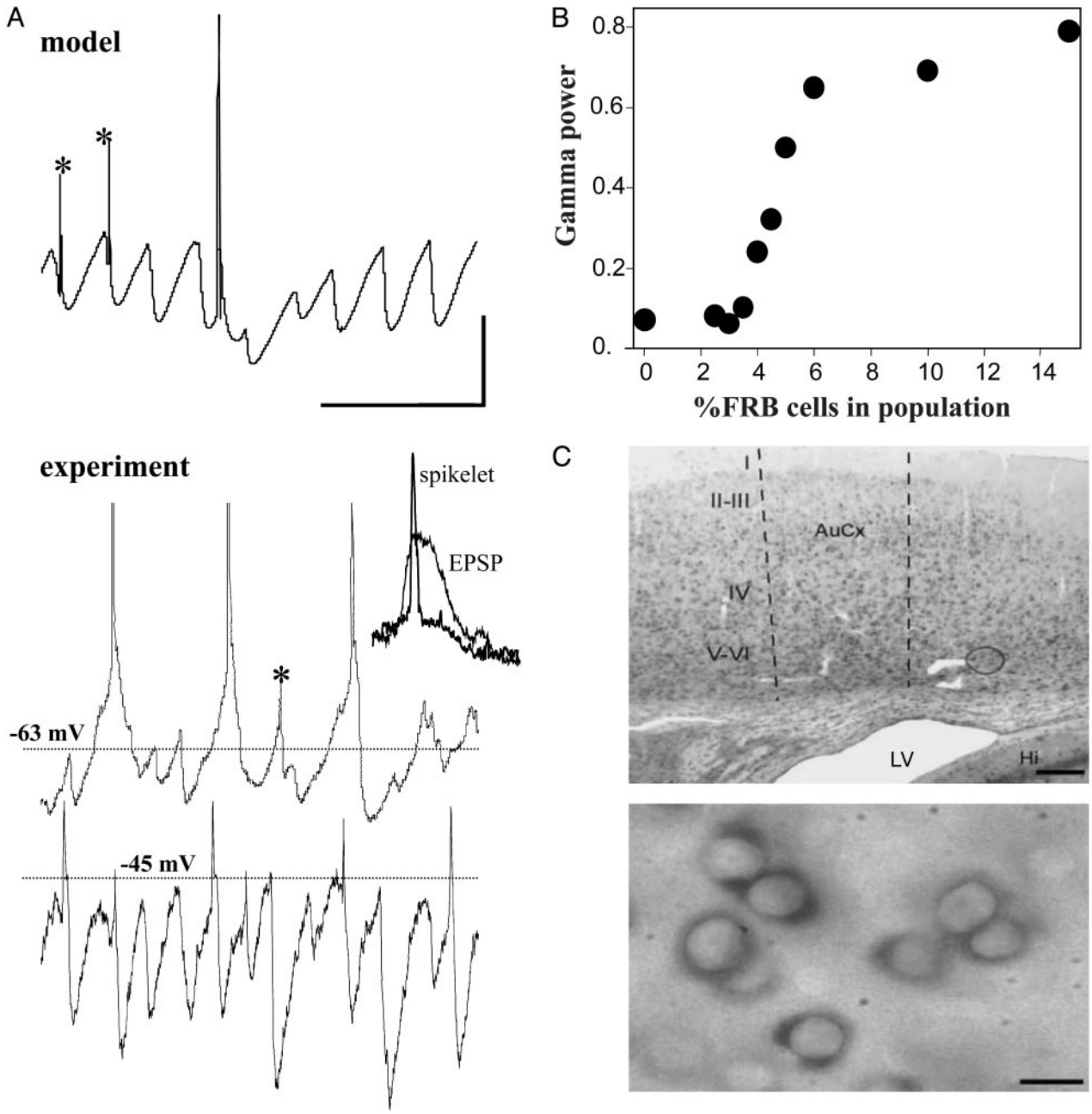

Fig. 2. RS cells fire sporadically but exhibit evidence of axonal activity, whereas FRB cells are predicted to help generate the gamma oscillation. (*A*) In both model and experiment, RS cells would on occasion exhibit spikelets at resting membrane potential during the oscillation (asterisks), having the appearance of miniature action potentials, and corresponding in the model to decrementally conducted antidromic spikes. Depolarization of RS cells to more than -50 mV abolished full somatic spikes but left spikelets intact (lower trace). (*Inset*) Shown are superimposed averages ($n = 10$) of RS cell spikelets and EPSPs to demonstrate differences in kinetics. Spikelets were not observed in FRB cells in either this model or experiment. Scale bars: 10 mV (model), 5 mV (experiment), and 100 ms (*Inset* 40 ms). (*B*) In contrast, the model predicts that FRB cells contribute to pacing the gamma rhythm. Gamma power rises as the percentage of FRB cells increases, with a threshold at $\approx$4% and leveling off of the power between $\approx$8% and 15% FRB cells. In these simulations, oscillation frequency ranged from 30.0 to 37.0 Hz, and was not correlated with the percent of FRB cells ($r^2 = 0.24$). (*C*) Evidence for a substrate for the sensitivity of the oscillation to gap-junction blockers has as yet to be found. However, mRNA for the gap-junction forming pannexin Px2 are present on neurons in auditory cortex. Shown are mRNA expression for Px2 by using nonradioactive *in situ* hybridization at low magnification (*Upper*: scale bar, 0.2 mm) and high magnification in LII-VI (*Lower*: scale bar, 10 μm).

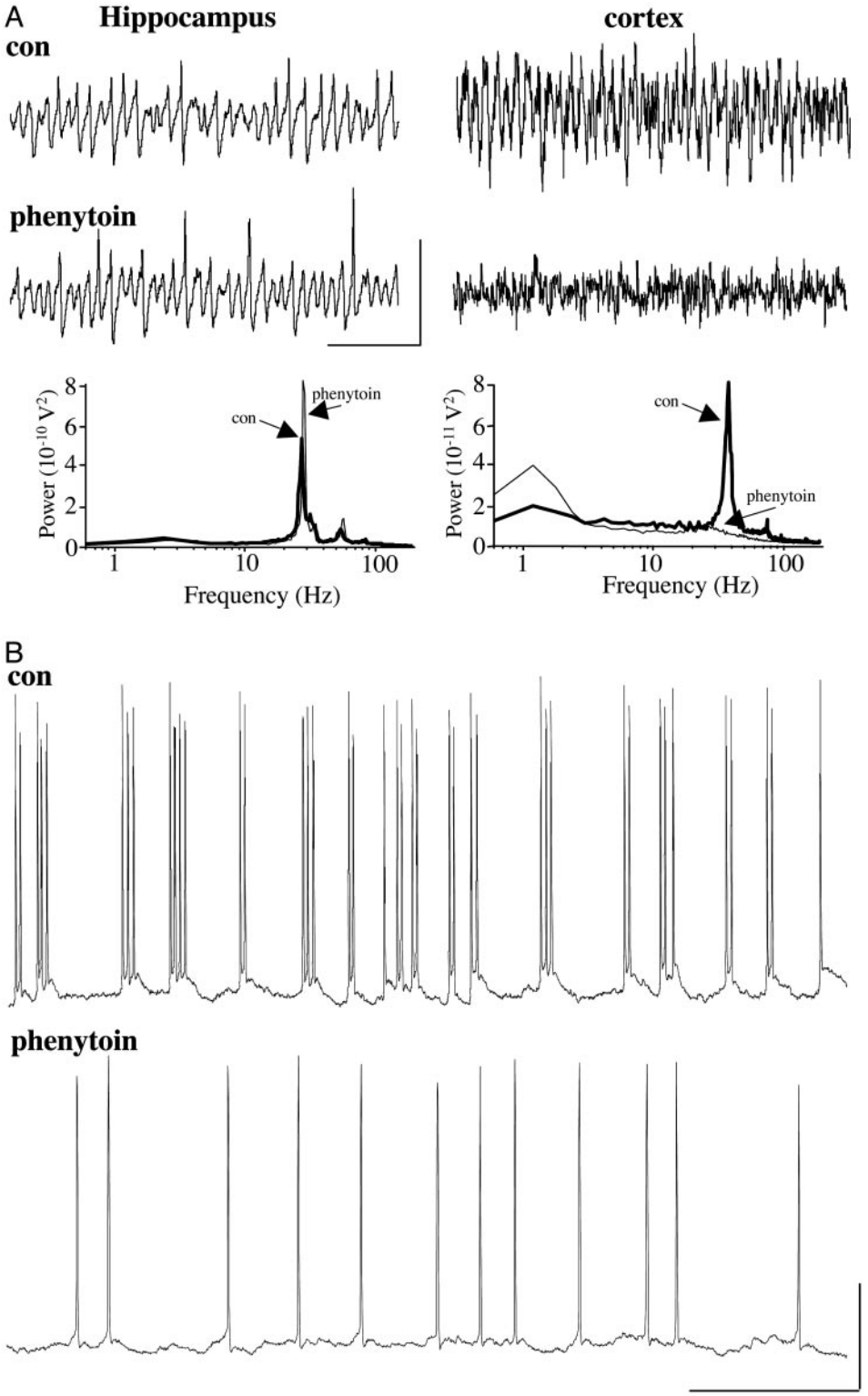

Fig. 3. Phenytoin blocks kainate-induced gamma oscillations in auditory cortex, but not in hippocampus, *in vitro*. (*A*) Field potential recordings (1-s epoch) of persistent gamma oscillations in the hippocampal CA3 stratum radiatum subfield (*Left*) and auditory cortical layer III (*Right*) are shown before (con) and after (phenytoin) bath application of 50 μM phenytoin. Scale bars: 0.5 mV (hippocampus), 0.1 mV (neocortex), 200 ms. Pooled mean power spectra (60-s epochs) show lack of significant effect of phenytoin on hippocampal persistent gamma ($n = 5$, $P > 0.05$), but abolition of neocortical gamma ($n = 6$). (*B*) Effects of phenytoin on FRB spike generation during kainate-induced gamma oscillations in neocortex. *Upper* shows 0.5-s epoch of FRB behavior in control conditions (field gamma present), and *Lower* shows single spiking in the same neuron after bath application of phenytoin (50 μM), at a time when field gamma was completely suppressed. Phenytoin (a blocker of persistent g_{Na}) suppressed FRB, and, because FRB cells are present in cortex but not in hippocampus, this finding suggests that FRB cells contribute to persistent gamma oscillations in cortex. [Note that phenytoin reduces persistent Na^+ conductance both in cortex (31) and in hippocampus (33).]

potentials (mostly inhibitory postsynaptic potentials, in both model and experiment, e.g., Fig. 2). Experimental values for mean number of spikes per wave were FS cells: 0.82 ± 0.11 (n = 5); LTS cells: 0.13 ± 0.05 (n = 6); FRB cells: 1.84 ± 0.26 (n = 4); and RS cells: 0.09 ± 0.02 (n = 10). Both in model and experiment, we found spikelets in some of the RS cells (Fig. 2*A*), but never in FRB cells experimentally. However, simulations showed that occasional spikelets could occur in FRB cells with lower tonic drive and altered network connectivity (data not shown). In the model, RS spikelets occurred on average at 2.2 Hz (12 cells) and corresponded to axonal spikes that conducted antidromically with decrement (ref. 27 and Fig. 2*A*), whereas axonal spikes in FRB cells mainly led to full spikes or multiplets, presumably because of the relative depolarization and altered intrinsic currents in FRB cells. Spikelets in RS cells were clearly distinct from EPSPs. First, their rise and decay times were some 10-fold faster than excitatory postsynaptic events (Fig. 2*A*). Second, depolarization of RS neurons led to an increase in spikelet amplitude, whereas EPSPs could no longer be seen above the inhibitory postsynaptic potential train. No evidence exists yet as to the substrate for spikelet formation. The model predicts that sharing of antidromic spikes by means of gap junctions in an axonal plexus may be responsible. Neuronal gap junctions in neocortex may be made up of connexin proteins (mainly connexin 36; ref. 18) or pannexins (14). Neurons in the superficial and deep layers of the primary auditory cortex contained large quantities of mRNA for pannexin 1 (data not shown) and pannexin 2 (Fig. 2*C*). Heteromeric hemichannels made up of pannexins 1 and 2 form functional ionophores when expressed in oocytes (14).

Given the multiple similarities between model and experiment, we used the model to try to predict how the presence of FRB neurons would affect gamma power (Fig. 2*B*). We found that a critical minimum of FRB cells needed to be present, ≈4% or 5% of the neuronal population with our parameter choices, to obtain a coherent gamma oscillation. This value was not statistically significant from the incidence of FRB cells derived from experimental data (four cells from 200 impalements, $P > 0.05$). We examined FRB percentages up to 15%, which is approximately the percentage of FRB neurons found in cat visual cortex *in vivo* (28), although even higher percentages have been reported under natural waking conditions (29). Peak gamma power leveled off, in our simulations, above ≈8% FRB cells. The threshold fraction of FRB cells required for coherent gamma is parameter-dependent: if the tonic depolarization of RS cells is elevated enough, then a gamma oscillation occurs with < 1% FRB neurons, although with a higher fraction of RS spikes per oscillation wave (data not shown).

If FRB cells are necessary for cortical gamma *in vitro*, one would predict that phenytoin, an anticonvulsant drug that blocks persistent sodium conductance, should suppress the oscillation. Because phenytoin suppresses FRB behavior (30, 31), and because FRB cells do not occur in hippocampus, this finding would suggest that FRB activity may be necessary for cortical gamma, but not for hippocampal gamma. This selective effect on gamma frequency oscillations was seen experimentally (Fig. 3*A*). Peak neocortical gamma power was reduced from 0.084 ± 0.013 nV^2 to 0.007 ± 0.002 nV^2 ($P < 0.05$, $n = 6$). Fig. 3*B* demonstrates that phenytoin indeed converts neocortical FRB behavior to RS, during bath application of kainate. As a control for effects on network components other than FRB neuronal spiking, we examined the effects of phenytoin on kainate-induced hippocampal persistent gamma oscillations, wherein FRB neurons have not been observed. Phenytoin did not suppress persistent gamma oscillations in hippocampus *in vitro*: mean gamma power went from 0.59 ± 0.12 nV^2 to 0.82 ± 0.34 nV^2 ($n = 5$, $P > 0.05$).

Discussion

The experimental observations demonstrated a profile of gamma frequency oscillations qualitatively similar to that seen in archicortex. The rhythm generated by kainate application consisted of trains of inhibitory postsynaptic potentials in principal cells and, with smaller amplitude, in interneurons. The rhythm depended on gap-junctional transmission, and ectopic spikes were seen in most RS neurons. Such ectopic spikes, along with electrical coupling between pyramidal neurons, lead to barrages of EPSPs in interneurons that are necessary for the oscillation in the hippocampus (19). This pattern of phasic excitation driving inhibition appears also to occur in the neocortex as blockade of phasic AMPA receptor-mediated excitation, and $GABA_A$ receptor-mediated synaptic inhibition also destroy the oscillation. The frequency of the field oscillation also depended on the kinetics of $GABA_A$ receptor-mediated synaptic events as was also seen for hippocampal gamma oscillations (4, 17). However, one striking difference between neocortical gamma oscillations and hippocampal gamma oscillations was the sensitivity to blockade of persistent sodium channels. The observation that FRB behavior could be concomitantly reduced with field gamma power in neocortex but not archicortex strongly suggested that FRB cells play a critical role in generating neocortical gamma. Blockade of FRB behavior still allowed FRB cells to generate rhythmic action potential outputs but, in the presence of phe-

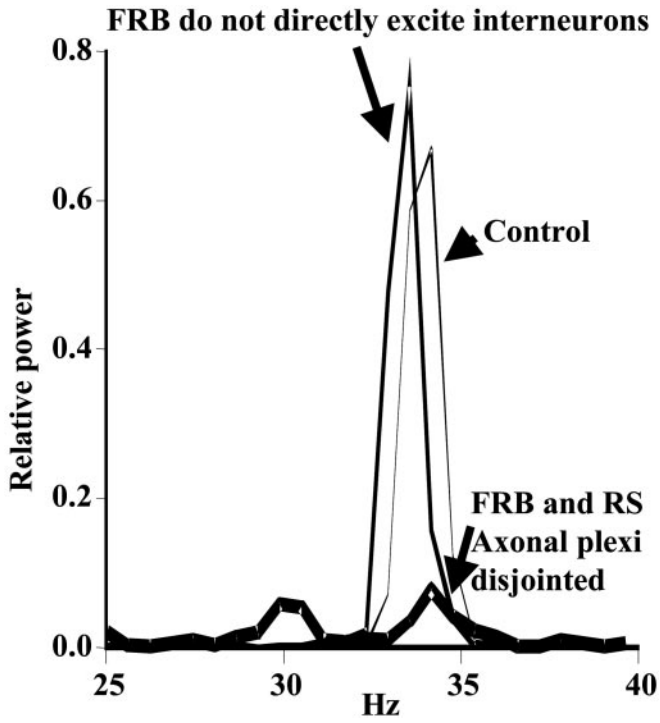

Fig. 4. FRB cells are predicted to generate field gamma oscillations through their electrical coupling with RS axons. Power spectra are shown for three simulations, each in a network with 6.5% FRB cells, and with blockade of recurrent synaptic excitation between pyramidal neurons (both RS and FRB). In the control run (i.e., no other manipulations), there is a large gamma peak, indicating that recurrent synaptic excitation between pyramidal cells is not required for the simulated oscillation. If, in addition, FRB neurons do not synaptically excite interneurons, there is still a large gamma peak. Hence, FRB cells can pace gamma activity without having any (chemical) synaptic output. In contrast, if FRB axons are not allowed to couple electrically with RS axons (but are allowed to couple with each other and directly synaptically excite interneurons), then the gamma oscillation is virtually abolished. Thus, in our model, the contribution of FRB cells to maintaining gamma is mediated by means of electrical coupling.

nytoin, only action potential singlets were seen, as opposed to (predominantly) multiplets in control conditions. Lowering the proportion of FRB cells in the model was also accompanied by a collapse in gamma power (Fig. 2*B*). These observations suggest that it is the large, high-frequency, barrage of output from FRB cells on many underlying gamma periods that is critical for their role in neocortical rhythmogenesis.

By what mechanism is this large FRB neuron output favoring gamma oscillations? The model, and observed experimental effects of the gap-junction blocker carbenoxolone, provided several suggestive insights. First, synaptic excitation of pyramidal cells (either RS or FRB) by the FRB cells (9) was not sufficient for the permissive effect of the FRB neurons in the model (control power spectrum in Fig. 4). Indeed, synaptic excitation of interneurons by FRB neurons (9) was also not sufficient (Fig. 4). The only other possible interaction in the model between FRB cells and other neurons is mediated by means of electrical coupling. Neurons in the auditory cortex strongly express mRNA for the px2 gap-junction-forming protein (Fig. 2*C*) that can form channels in conjunction with px1 (14), which is also present (data not shown), but as yet, a substrate for axonal gap junctions in this region remains elusive. However, we reconfigured the network so that no electrical couplings occurred between FRB/RS axonal pairs, while maintaining the total number of pyramidal cell electrical couplings constant. In this case, even with 6.5% of pyramidal cells being FRB cells, and with synaptic connections between FRB cells and interneurons intact, the gamma oscillation collapsed (Fig. 4). Hence, in the model, FRB neurons exerted a permissive effect on gamma oscillations because their axons were electrically coupled not only with each other, but also with RS axons (and *vice versa*).

In conclusion, our combined experimental/simulation study demonstrated that field gamma oscillations depended on expression of FRB in a small subset of cortical neurons. The reduction in gamma power by the gap-junction blocking agent carbenoxolone suggested that the axons of layer II/III are electrically coupled, as appears to be the case for pyramidal neurons in hippocampus (27, 32). Finally, although not a comprehensive computational model of neocortical networks as yet, the model predicted accurately the physiological and pharmacological experimental data presented, and suggested that RS neurons and FRB neurons are electrically interconnected, and that such interconnections are critical for persistent neocortical gamma oscillations.

We thank Robert Walkup of the IBM T.J. Watson Research Center (Yorktown Heights, NY) for assistance with parallel computing. This work was supported by National Institute of Neurological Disorders and Stroke/National Institutes of Health, Volkswagen Stiftung, Medical Research Council (United Kingdom), and the Wellcome Trust.

1. Tallon-Baudry, C. & Bertrand, O. (1999) *Trends Cogn. Sci.* **4,** 151–162.
2. Engel, A. K., König, P., Gray, C. M. & Singer, W. (1990) *Eur. J. Neurosci.* **7,** 588–606.
3. Engel, A. K. & Singer, W. (2001) *Trends Cogn. Sci.* **1,** 16–25.
4. Whittington, M. A., Traub, R. D. & Jefferys, J. G. (1995) *Nature* **373,** 612–615.
5. Cunningham, M. O., Davies, C. H., Buhl, E. H., Kopell, N. & Whittington, M. A. (2003) *J. Neurosci.* **23,** 9761–9769.
6. Whittington, M. A., Traub, R. D., Kopell, N., Ermentrout, B. & Buhl, E. H. (2000) *Int. J. Psychophysiol.* **38,** 315–336.
7. Varela, F. J. (1995) *Biol. Res.* **28,** 81–95.
8. Gray, C. M. & McCormick, D. A. (1996) *Science* **274,** 109–113.
9. Steriade, M., Timofeev, I., Dürmüller, N. & Grenier, F. (1998) *J. Neurophysiol.* **79,** 483–490.
10. Steriade, M. (2001) *The Intact and Sliced Brain* (MIT Press, Cambridge, MA).
11. Llinás, R. R., Grace, A. A. & Yarom, Y. (1991) *Proc. Natl. Acad. Sci. USA* **88,** 897–901.
12. Tamás, G., Buhl, E. H. & Somogyi, P. (1997) *J. Physiol. (London)* **500,** 715–738.
13. Grenier, F., Timofeev, I. & Steriade, M. (2003) *J. Neurophysiol.* **89,** 841–852.
14. Bruzzone, R., Hormuzdi, S. G., Barbe, M., Herb, A. & Monyer, H. (2003) *Proc. Natl. Acad. Sci. USA* **100,** 13644–13649.
15. Catania, M. A., Tolle, T. R. & Monyer, H. (1995) *J. Neurosci.* **15,** 7046–7061.
16. Buhl, E. H., Tamás, G. & Fisahn, A. (1998) *J. Physiol. (London)* **513,** 117–126.
17. Fisahn, A., Pike, F. G., Buhl, E. H. & Paulsen, O. (1998) *Nature* **394,** 186–189.
18. Hormuzdi, S. G., Pais, I., LeBeau, F. E., Towers, S. K., Rozov, A., Buhl, E. H., Whittington, M. A. & Monyer, H. (2001) *Neuron* **31,** 487–495.
19. Traub, R. D., Cunningham, M. O., Gloveli, T., LeBeau, F. E. N., Bibbig, A., Buhl, E. H. & Whittington, M. A. (2003) *Proc. Natl. Acad. Sci. USA* **100,** 11047–11052.
20. Traub, R. D., Buhl, E. H., Gloveli, T. & Whittington, M. A. (2003) *J. Neurophysiol.* **89,** 909–921.
21. Traub, R. D., Pais, I., Bibbig, A., LeBeau, F. E. N., Buhl, E. H., Hormuzdi, S. G., Monyer, H. & Whittington, M. A. (2003) *Proc. Natl. Acad. Sci. USA* **100,** 1370–1374.
22. Galarreta, M. & Hestrin, S. (1999) *Nature* **402,** 72–75.
23. Gibson, J. R., Beierlein, M. & Connors, B. W. (1999) *Nature* **402,** 75–79.
24. Venance, L., Rozov, A., Blatow, M., Burnashev, N., Feldmeyer, D. & Monyer, H. (2000) *Proc. Natl. Acad. Sci. USA* **97,** 10260–10265.
25. Tamás, G., Buhl, E. H., Lörincz, A. & Somogyi, P. (2000) *Nat. Neurosci.* **3,** 366–371.
26. Traub, R. D., Bibbig, A., Fisahn, A., LeBeau, F. E. N., Whittington, M. A. & Buhl, E. H. (2000) *Eur. J. Neurosci.* **12,** 4093–4106.
27. Schmitz, D., Schuchmann, S., Fisahn, A., Draguhn, A., Buhl, E. H., Petrasch-Parwez, R. E., Dermietzel, R., Heinemann, U. & Traub, R. D. (2001) *Neuron* **31,** 831–840.
28. Nowak, L. G., Azouz, R., Sanchez-Vives, M. V., Gray, C. M. & McCormick, D. A. (2003) *J. Neurophysiol.* **89,** 1541–1566.
29. Steriade, M., Timofeev, I. & Grenier, F. (2001) *J. Neurophysiol.* **85,** 1969–1985.
30. Lampl, I., Schwindt, P. & Crill, W. (1998) *J. Pharmacol. Exp. Ther.* **284,** 228–237.
31. Brumberg, J. C., Nowak, L. G. & McCormick, D. A. (2000) *J. Neurosci.* **20,** 4829–4843.
32. Draguhn, A., Traub, R. D., Schmitz, D. & Jefferys, J. G. R. (1998) *Nature* **394,** 189–192.
33. Segal, M. M. & Douglas, A. F. (1997) *J. Neurophysiol.* **77,** 3021–3034.